environmental microbiology

Environmental Microbiology (2012) **14**(8), 1982–1994 doi:10.1111/j.1462-2920.2012.02741.x

High cellular organization of pyoverdine biosynthesis in *Pseudomonas aeruginosa*: clustering of PvdA at the old cell pole

Laurent Guillon,[1] Maher El Mecherki,[1] Stephan Altenburger,[2] Peter L. Graumann[2] and Isabelle J. Schalk[1]*

[1]*UMR 7242, Université de Strasbourg-CNRS, ESBS, Blvd Sébastien Brant, F-67413 Illkirch, Strasbourg, France.*

[2]*Mikrobiologie, Fachbereich für Biologie, Universität Freiburg, Schänzle Straße 1, 79104 Freiburg, Germany.*

Summary

Pyoverdine I (PVDI) is the major siderophore produced by *Pseudomonas aeruginosa* PAO1 to import iron. Its biosynthesis requires the coordinated action of cytoplasmic, periplasmic and membrane proteins. The individual enzymatic activities of these proteins are well known. However, their subcellular distribution in particular areas of the cytoplasm, periplasm, or within the membrane has never been investigated. We used chromosomal replacement to generate *P. aeruginosa* strains producing fluorescent fusions with PvdA, one of the initial enzymes in the biosynthetic pathway of PVDI in the cytoplasm, and PvdQ, involved in the maturation of PVDI in the periplasm. Cellular fractionation indicated that a substantial amount of PvdA-YFP was located in the membrane fraction. Epifluorescence microscopy imaging showed that PvdA-YFP was mainly clustered at the old cell pole of bacteria, indicating a polar segregation of the protein. Epifluorescence and TIRF imaging on cells expressing labelled PvdQ showed that this enzyme was uniformly distributed in the periplasm, in contrast with PvdA-YFP. The description of the intracellular distribution of these enzymes contributes to the understanding of the PVDI biosynthetic pathway.

Introduction

Iron acquisition challenges bacteria, as almost all living organisms, because this metal is on the one hand a cofactor of numerous redox-dependent key enzymes and on the other hand is poorly bioavailable. As a consequence, bacteria have evolved biosynthetic pathways to produce and secrete high-affinity sequestrating agents called siderophores. These molecules efficiently chelate iron in the bacterial environment such that it can be transported back into the microorganism (Boukhalfa and Crumbliss, 2002; Braun and Hantke, 2011; Hider and Kong, 2011).

The opportunistic Gram-negative bacterium *Pseudomonas aeruginosa* secretes a fluorescent siderophore called pyoverdine (PVDI) (Meyer and Abdallah, 1978; Schalk, 2008). This chelator is composed of three parts: (i) a chromophore derived from 2,3-diamino-6,7-dihydroxyquinoline, (ii) a peptide moiety consisting of eight amino acids bound to the carboxylic group of the chromophore and (iii) a dicarboxylic acid or dicarboxylic amide attached to the C-3 of the chromophore (Demange *et al.*, 1990). PVDI synthesis starts in the cytoplasm with the synthesis of a non-fluorescent precursor (Hannauer *et al.*, 2012) and ends in the periplasm (Yeterian *et al.*, 2010a). The backbone of PVDI is assembled in the cytoplasm and requires the coordinated activity of four large cytoplasmic modular enzymes known as nonribosomal peptide synthetases (NRPSs) – PvdL, PvdI, PvdJ and PvdD (Mossialos *et al.*, 2002; Ackerley *et al.*, 2003; Ravel and Cornelis, 2003) – and enzymes producing the substrates for the four NRPSs (Visca *et al.*, 2007). PvdA, a L-ornithine hydroxylase, and PvdF, a hydroxyornithine transformylase, catalyse the transformation of L-ornithine into L-formyl-N^{δ}-hydroxyornithine, which is a substrate for the NRPSs, PvdI and PvdJ (McMorran *et al.*, 2001; Meneely *et al.*, 2009). PvdH, an amidotransferase, converts the L-aspartate β-semialdehyde into L-2,4-diaminobutyrate, which is then incorporated into the peptide chain by PvdL (Vandenende *et al.*, 2004). The PVDI synthesis starts with PvdL, which couples coenzyme A to a myristic acid in an ATP-dependent reaction and delivers it to the L-Glu residue in the second domain of PvdL (Mossialos *et al.*, 2002; Gulick and Drake, 2011). After incorporation of the first three residues – L-Glu, L-Tyr and L-Dab – the other amino-acid residues are incorporated by PvdI (for L-Ser, L-Arg, L-Ser and L-OHOrn), PvdJ (for L-Lys and L-OHOrn), and PvdD (for

Received 24 November, 2011; revised 9 March, 2012; accepted 10 March, 2012. *For correspondence. E-mail isabelle.schalk@unistra.fr; Tel. (+33) 3 68 85 47 19; Fax (+33) 3 68 85 48 29.

the two L-Thr) (Visca *et al.*, 2007). The presence of a myristic group on the first residue (L-Glu) probably keeps the PVDI precursor at the inner membrane throughout the biosynthetic process (Hannauer *et al.*, 2012).

After formation of the PVDI backbone, which is non-fluorescent and has a mysristic group on the L-Glu residue (Hannauer *et al.*, 2012), the precursor is transported across the inner membrane by an export ABC transporter PvdE (Hannauer *et al.*, 2010) and the subsequent biosynthetic steps occur in the periplasm. Biochemical and crystallographic studies suggested that PvdQ, an N-terminal nucleophile hydrolase (Ntn-hydrolase), is involved in the excision of the fatty-acid chain (Gulick and Drake, 2011; Hannauer *et al.*, 2012). This is then followed by the cyclization of the chromophore, which yields the fluorescent PVDI. The periplasmic enzymes (PvdN, PvdO and PvdP) (Ravel and Cornelis, 2003; Lewenza *et al.*, 2005), necessary for PVDI production (Ochsner *et al.*, 2002; Lamont and Martin, 2003; Voulhoux *et al.*, 2006; Yeterian *et al.*, 2010a), are probably implicated in this step. Mutation of PvdN and PvdP abolish the secretion of fluorescent PVDI, indicating that these proteins must be involved in PVDI chromophore formation (Yeterian *et al.*, 2010a). The efflux pump PvdRT-OpmQ has been implicated in the delivery of newly synthesized PVDI from the periplasm into the extracellular medium (Hannauer *et al.*, 2010).

The activities of various enzymes involved in PVDI biosynthesis in *P. aeruginosa* have been described. However, it is hard to imagine how this highly complex mechanism, with sequential steps in all cell compartments, is orchestrated to efficiently yield a mature complex siderophore. Over the past decade, numerous GFP-tagged proteins have been identified at specific intracellular locations such as the poles of the cells, indicating that bacteria have a degree of intracellular organization (Shapiro *et al.*, 2009). Processes such as bacterial cell cycle, motility and development are now understood to depend upon the specific distribution of proteins within the cytoplasm or within the membrane (Dworkin, 2009; Shapiro *et al.*, 2009; Rudner and Losick, 2010). These specific cell locations are critical for bacterial cell physiology. To further understand how these cellular locations influence PVDI biosynthesis, we generated *P. aeruginosa* mutant strains expressing, at native levels, proteins involved in this process fused with either eYFP or mCHERRY. We focused on PvdA, as one of the initial enzymes in the biosynthetic pathway of PVDI in the cytoplasm, and PvdQ, as the best characterized protein involved in the maturation of PVDI in the periplasm before secretion. We showed that PvdA and PvdQ, which are involved in two very distant steps in the PVDI biosynthetic pathway, had completely different distributions within the cell. Whereas PvdA was mainly located at the old cell pole, PvdQ was uniformly distributed throughout the periplasm.

Results

The PvdA C-terminal fusion is functional whereas the N-terminal fusion is not

Our aim was to localize the PvdA enzyme in its intracellular environment, when expressed at physiological levels. We constructed suicide vectors containing DNA encoding eYFP flanked by 700 bp upstream and downstream to the insertion sites. Insertion of these modified regions by allelic exchange into wild-type PAO1 (Ye *et al.*, 1995) produced two strains expressing eYFP fused either at the N-terminus (*yfp-pvdA*) or the C-terminus (*pvdA-yfp*) of PvdA.

PVDI has a characteristic absorbance at 447 nm. We thus monitored bacterial growth (by measuring the optical density at 600 nm) and PVDI production (by measuring the optical density at 400 nm) over time for PAO1, PAO1*pvdA*, *yfp-pvdA* and *pvdA-yfp* in iron-depleted minimal media (Fig. 1A). As previously reported, deletion of the *pvdA* gene did not affect bacterial growth but did abolish PVDI production (Visca *et al.*, 1994; Ochsner *et al.*, 2002; Lamont and Martin, 2003). Concerning our insertion mutants, *pvdA-yfp* synthesized PVDI at the same level as wild-type PAO1, whereas expression of PVDI was not detected in *yfp-pvdA*. We also tested the ability of *yfp-pvdA* and *pvdA-yfp* to transport Pvd-^{55}Fe complexes. As expected, both of these strains transported PVDI-^{55}Fe complexes as efficiently as the PAO1 and the PAO1*pvdA* deletion strains (data shown in Fig. S1A in *Supporting information* for *pvdA-yfp*).

The PvdA C-terminal fusion is stable whereas the N-terminal fusion is not expressed

To check the integrity of the PvdA fusion proteins, we subjected whole-cell extracts from PAO1, PAO1*pvdA*, *yfp-pvdA* and *pvdA-yfp* cultures to SDS-PAGE electrophoresis followed by Western blot analysis using anti-GFP antibodies, which can detect all variants of *Aequorea victoria* GFP. As expected, no eYFP signal was detected in the PAO1 or the PAO1*pvdA* strains. A single band below the 100 kDa marker band was detected in the cell extracts from the *pvdA-yfp* strain (Fig. 2A). Because wild-type PvdA migrates at an apparent mass of ~49 kDa (Imperi *et al.*, 2008), the band detected in the *pvdA-yfp* strain is consistent with an insertion of the eYFP protein into PvdA, which would generate an ~80 kDa PvdA-eYFP fusion protein. In contrast, no eYFP was detected in the cell extracts from the *yfp-pvdA*, indicating that no eYFP is expressed in this N-terminal fusion strain. It is therefore

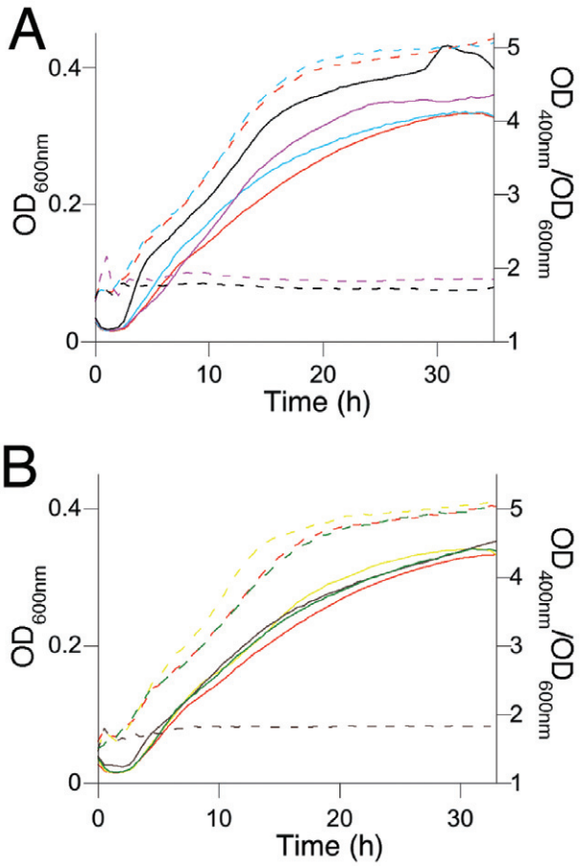

Fig. 1. Effect of fusion proteins of eYFP with PvdA (A) and of mCHERRY with PvdQ (B) on bacterial growth and PVDI production. Bacteria were washed in iron-depleted succinate media to remove iron from LB media. Fresh minimal media were then inoculated with these bacteria and distributed into a 96-well plate. The growth (solid lines in panels A and B) and PVDI production (dashed lines in panels A and B) were monitored over time by OD_{600} and OD_{400} measurements. Panel (A) presents the measurements for PAO1 (red), PAO1*pvdA* (black), *yfp-pvdA* (pink), and *pvdA-yfp* (blue) and panel (B) for PAO1 (red), PAO1*pvdQ* (brown), *mcherry-pvdQ* (green), and *pvdQ-mcherry* (yellow). These measurements were performed every 30 min in a Tecan microplate reader with shaking and incubation at 30°C. Each curve represents a mean derived from six replicates. PVDI production (OD_{400}) at a given time was normalized by the corresponding bacterial-growth reading (OD_{600}).

highly likely that the PAO1*pvdA* phenotype of *yfp-pvdA* is due to the absence of the fusion protein eYFP-PvdA rather than a defect in enzymatic activity.

PvdA is a membrane-associated protein located at the old cell pole

pvdA-yfp strain was used to investigated the *in vivo* subcellular location of PvdA using cell fractionation. We analysed each fraction, exploiting the fluorescence of eYFP to detect the PvdA fusion protein and the fluorescence of PVDI to assess the fractionation efficiency – as PVDI is located in the periplasm (Greenwald *et al.*, 2007; Yeterian *et al.*, 2010a). As a control, we checked that no eYFP was detected in the cellular compartments of a PAO1 strain. As shown in Fig. 2B, 82% of the total PVDI fluorescence was detected in the periplasm of *pvdA-yfp*, indicating a successful fractionation. In contrast, eYFP was predominantly detected in the membrane fraction, which contained 60% of the total eYFP fluorescences, compared with 36% of the total eYFP fluorescence contained in the cytoplasm. This is consistent with previous

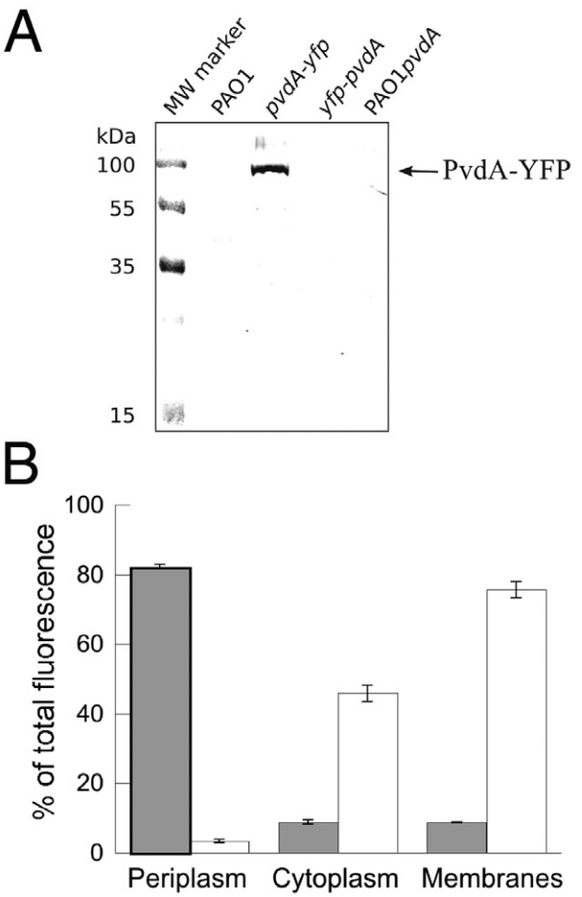

Fig. 2. A. Immunoblot analysis of the PAO1, PAO1*pvdA*, *yfp-pvdA* and *pvdA-yfp* strains. The equivalent of 0.25 OD_{600} units of each strain grown in succinate media were lysed in loading buffer, DNA digested by benzonase (1 U), and loaded onto SDS-PAGE for protein separation. Proteins were blotted onto a nitrocellulose membrane and eYFP was detected using anti-GFP antibodies. Molecular weight (MW) marker bands are indicated on the left.
B. Cell fractionation of the *pvdA-yfp* strain. Cell fractionation was performed as described in *Experimental procedures*. The intensity of the fluorescent signal corresponding to PVDI (grey columns) and eYFP (white columns) was measured in parallel for equal volumes of the cytoplasmic, periplasmic, and cell-membrane fractions. The data shown represent the means of three independent experiments.

reports that wild-type PvdA is mostly found associated with membranes (Imperi *et al*., 2008).

We then assessed the *in vivo* protein location using epifluorescence imaging of the *pvdA-yfp* strain grown in minimal media. During the stationary phase, we found that PvdA-YFP was mainly located on one pole of the cells. It is therefore possible that the membrane-associated PvdA-YFP formed a patch on the membrane, whereas we observed that the cytoplasmic fraction of PvdA-eYFP was uniformly distributed. We monitored the evolution of the cells containing a fluorescence spot over the unspotted cell throughout cell growth. Although no spotted cells could be detected during the lag phase or at the beginning of the exponential phase, we observed the first patches of fluorescence during the mid-exponential phase and the number of spotted PvdA-eYFP cells increased until the stationary phase, when all of the cells displayed a patched pattern (Fig. 3A). Lifetime imaging showed that this patch of PvdA-YFP was located at the old pole of the mother cell during division (Fig. 3B). As expected, when PvdA-YFP was found to be uniformly distributed throughout the cytoplasm, the protein appeared to be equally distributed to the daughter cells (Fig. 3C). In the presence of 10 μM PVDI-Fe, no fast dissolution of the PvdA-YFP spots in *pvdA-yfp* cells was observed. The spots only started to disappear after completion of a cell cycle (Fig. 3D). In conclusion, PvdA-YFP was mainly located in clusters at the old cell pole, and exhibited a polar distribution following cell division, whereas a subset of cells displayed a uniform distribution of the fusion protein within the cytoplasm.

PvdQ N- and C-terminal fusions are fully active

We then focused on the PvdQ enzyme to gain insights into the periplasmic maturation of PVDI. PvdQ belongs to the superfamily of the N-terminal nucleophile hydrolases (Ntn-hydrolases). Although proteins from this family possess various enzymatic activities, all exhibit an auto-proteolytic activation resulting in the formation of two tightly bound chains (an α-subunit of 18 kDa that comes from the N-terminal domain of the proenzyme and a 60 kDa β-chain) and the creation of an active site (Oinonen and Rouvinen, 2000; Sio *et al*., 2006). To determine the subcellular location of PvdQ, we inserted DNA encoding mCHERRY by allelic exchange to generate mutant PAO1 strains expressing PvdQ with mCHERRY fused at either the N-terminus (*mcherry-pvdQ*) or the C-terminus (*pvdQ-mcherry*) of the protein. The insertion site for the N-terminal fusion was placed at alanine 23, which is downstream to the cleavage site of the signal sequence (Sio *et al*., 2006). Corresponding mutator vectors were constructed as described for the PvdA mutant strains.

We monitored bacterial growth and PVDI production for *mcherry-pvdQ*, *pvdQ-mcherry*, PAO1 and PAO1*pvdQ* strains, when cultured in iron-deficient succinate media (Fig. 1B). Every strain displayed similar growth profiles and only the PAO1*pvdQ* strain did not produce PVDI as described previously (Ochsner *et al*., 2002; Lamont and Martin, 2003; Nadal Jimenez *et al*., 2010), indicating that mCHERRY-PvdQ and PvdQ-mCHERRY retained wild-type PvdQ activity for PVDI production. As expected, the *mcherry-pvdQ* and *pvdQ-mcherry* mutant strains incorporated radiolabelled PVDI-Fe complex with the same efficiency as the PAO1 and PAO1*pvdQ* strains (Fig. S1B in *Supporting information*).

PvdQ has been recently shown to play a major role in biofilm formation in iron-depleted media (Wang *et al*., 2011). We tested the ability of the *mcherry-pvdQ* and *pvdQ-mcherry* strains to form biofilm (Fig. S2 in *Supporting information*). Both strains produced about the same amount of biofilm compared with the PAO1 strain, and produced significantly more biofilm than the PAO1*pvdQ* deletion mutant.

PvdQ N- and C-terminal fusions are stable and mCHERRY is attached to the α- or β-subunit of PvdQ respectively

We tested for the presence of the PvdQ-mCHERRY fusion proteins by immunoblot analysis on whole-cell extracts derived from PAO1, PAO1*pvdQ*, *mcherry-pvdQ* and *pvdQ-mcherry* strains grown in iron-depleted minimal media. Detection was performed using antibodies raised against PvdQ (Fig. 4A) or DsRed (Fig. 4B), which recognizes the mCHERRY protein. As expected, no signal for anti-PvdQ antibodies was observed in the PAO1*pvdQ* strain. In the extracts from the PAO1 strain, a single band of ~60 kDa was detected, which corresponds to the β-subunit of the PvdQ protein (Nadal Jimenez *et al*., 2010) (Fig. 4A). This same band was also observed for *mcherry-pvdQ* strain. A band of ~100 kDa was detected in the extracts from *pvdQ-mcherry*, which is consistent with the presence of an intact β-subunit of PvdQ fused to mCHERRY (Fig. 4A). Immunoblotting using anti-DsRed antibodies to detect mCHERRY yielded no signal in the extracts from PAO1 and PAO1*pvdQ*. However, anti-DsRed antibodies detected the same ~ 100 kDa band as that detected by anti-PvdQ antibodies in extracts from the *pvdQ-mcherry* strain, which corresponded to mCHERRY fused with the β-subunit of PvdQ (Fig. 4B). By comparing the signals for free mCHERRY (~ 30 kDa) and the ~ 50 kDa band detected in the *mcherry-pvdQ* strain, we deduced that when the PvdQ protein is matured, mCHERRY remains fused to the α-subunit (Fig. 4B). In conclusion, the fully active fusion proteins that we designed are mature in a similar manner to their wild-type

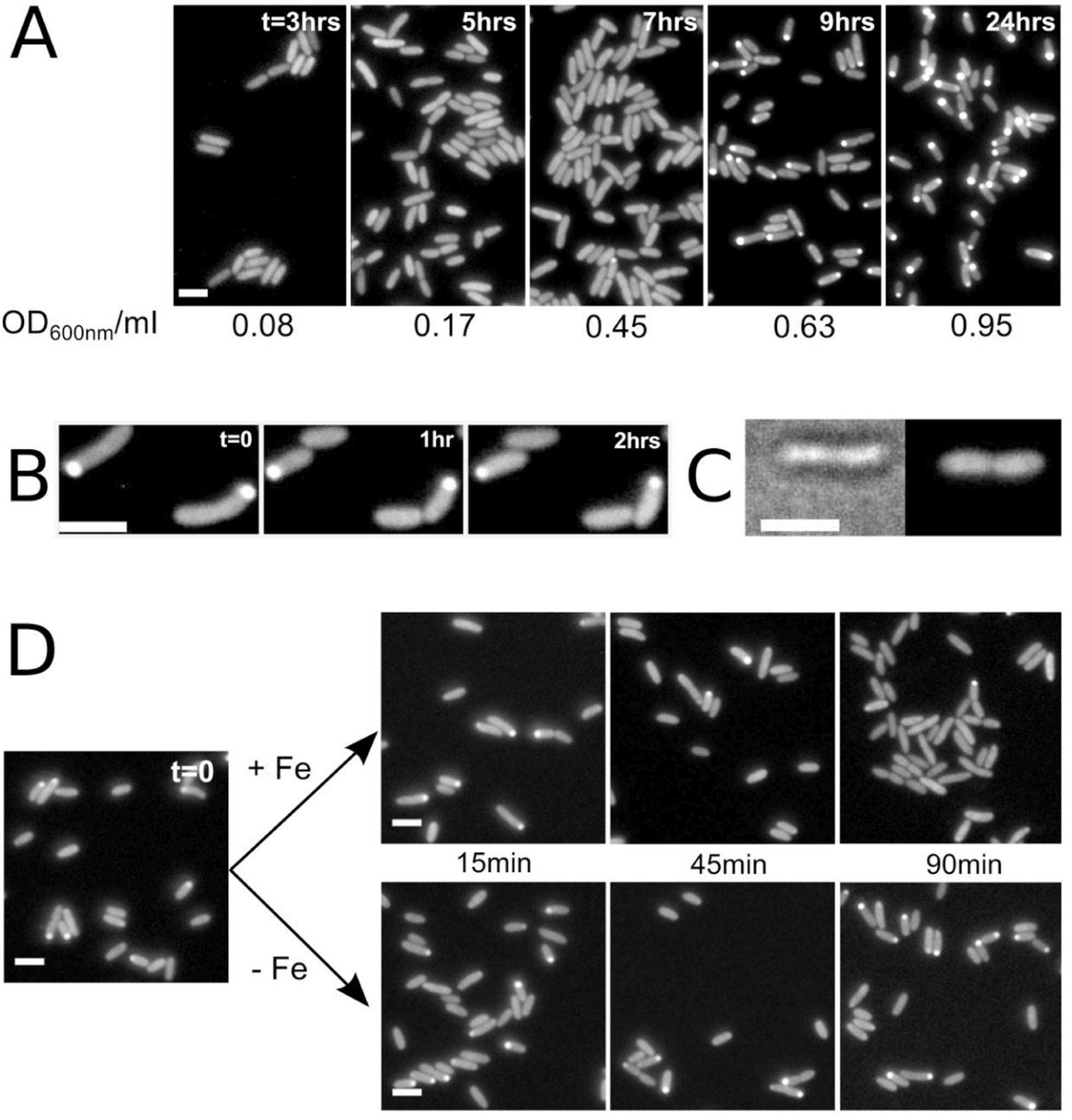

Fig. 3. A. Time-lapse fluorescence microscopy images of *pvdA-yfp* at different stages of bacterial growth. Cells were grown in minima media. At different times, aliquots were removed, cells spotted onto slides coated with agarose dissolved in minimal media and observed by fluorescence microscopy.
B. Time-lapse fluorescence microscopy images of the *pvdA-yfp* strain. Cell division was monitored on the *pvdA-yfp* strain, grown in minimal media. At mid-exponential phase, cells were spotted onto slides coated with agarose that was dissolved in minimal media. Images after 0, 1 and 2 h incubation of the slides at 30°C were recorded.
C. Unspotted *pvdA-yfp* cell division imaging by fluorescence microscopy (right) and brightfield (left).
D. Time-lapse fluorescence microscopy images of the *pvdA-yfp* strain in the presence and absence of 10 μM PVDI-Fe. At mid-exponential phase, cells grown in minima media were incubated in the presence or absence of PVDI-Fe. At different times, aliquots were removed and observed by fluorescence microcopy. All images were recorded using a filter set for eYFP imaging (scale bar 2 μm).

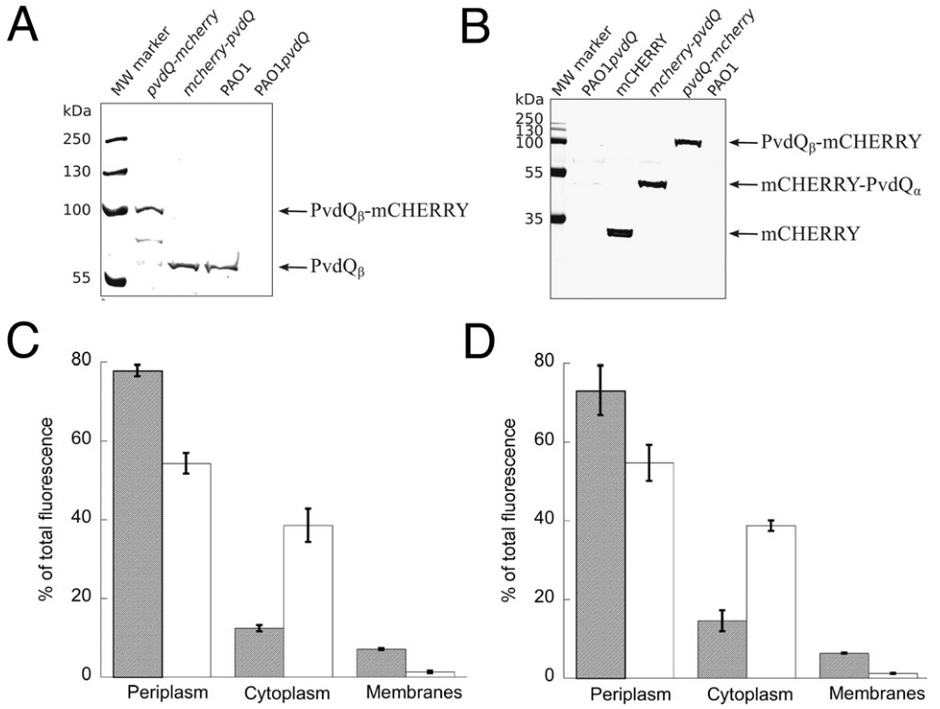

Fig. 4. A and B. Immunoblot analysis of the PAO1, PAO1*pvdQ*, *mcherry-pvdQ* and *pvdQ-mcherry* strains. The equivalent of 0.25 OD_{600} units of each strain grown in succinate media were lysed in loading buffer, DNA digested by benzonase (1 U), and loaded onto SDS-PAGE for protein separation. Proteins were blotted onto a nitrocellulose membrane and PvdQ was detected using anti-PvdQ antibodies (A) or anti-DsRed antibodies to detect mCHERRY (B). Molecular weight (MW) marker bands are indicated on the left.
C and D. Cellular fractionation of *mcherry-pvdQ* (C) and *pvdQ-mcherry* (D) strains. Fluorescence of PVDI (grey columns) and mCHERRY (white columns) were measured for equal volumes of the cytoplasmic, periplasmic and cell-membrane fractions. The data shown represent the means of three independent experiments.

counterparts, and mCHERRY is fused with the α-subunit of PvdQ in mCHERRY-PvdQ, and with the β-subunit of PvdQ in PvdQ-mCHERRY.

Periplasmic PvdQ fusion proteins are uniformly distributed within the periplasm

We performed cell-fractionation studies to confirm the export of the fusion proteins to the periplasm. *mcherry-pvdQ* and *pvdQ-mcherry* strains were cultured in succinate media and cytoplasmic, periplasmic, and membrane fractions were isolated. Very low levels of PVDI were detected in the cytoplasm (~ 13% of the total PVDI fluorescence), indicating that there was no significant periplasmic contamination of the cytoplasmic fractions (Fig. 4C and D). As expected from the PVDI-production phenotypes for mCHERRY-PvdQ and PvdQ-mCHERRY, most of the fluorescence for mCHERRY (54% of the total fluorescence for mCHERRY for both fusion proteins) was found in the periplasm (Fig. 4C and D). Nevertheless, a high level of fluorescence for mCHERRY (39% the total fluorescence for mCHERRY) was also observed in the cytoplasmic fraction for both fusion proteins. According to the cell fractionation of PVDI, the presence of mCHERRY in the cytoplasmic fractions is not due to periplasmic contamination. We compared the distribution of PvdQ in the cytoplasm and periplasm of the wild-type PAO1 strain with that of our mutants by immunoblot analysis using an anti-PvdQ antibody on the isolated cell compartments (Fig. S3 in *Supporting information*). Although similar amounts of the PvdQ β-chain were detected in both periplasmic and cytoplasmic fractions, the band corresponding to the PvdQ α-chain was detected in the periplasmic fraction only. Thus, the PvdQ enzyme in the cytoplasm may correspond to the uncleaved inactive form of the protein, which has yet to be exported to the periplasm to complete its full maturation. Finally, the distribution of PvdQ in the cytoplasm and periplasm of the *mcherry-pvdQ* and *pvdQ-mcherry* strains, was similar to that in the PAO1 strain. N- and C-terminal fusion proteins of mCHERRY and PvdQ therefore showed the same subcellular distribution as wild-type PvdQ.

The periplasmic fluorescence distributions in *mcherry-pvdQ* and *pvdQ-mcherry* strains were examined using epifluorescence microscopy. mCHERRY imaging identi-

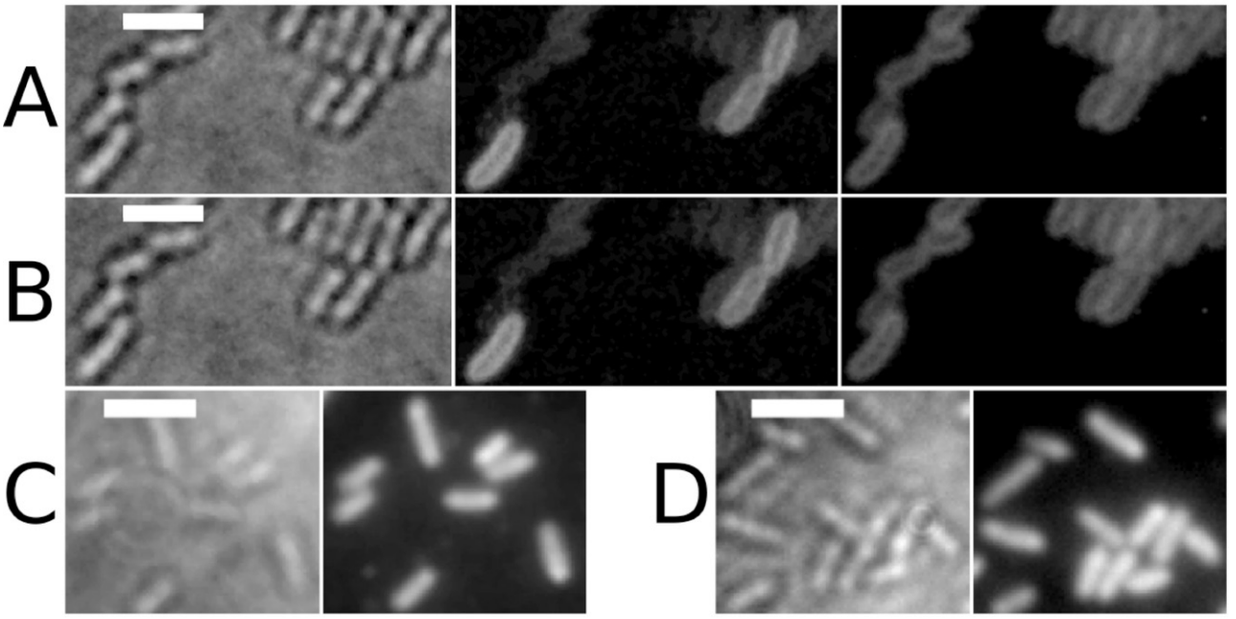

Fig. 5. A and B. Fluorescence microscopy images of *mcherry-pvdQ* (A) and *pvdQ-mcherry* strains (B). From left to right, brightfield, PVDI and mCHERRY epifluorescence images (scale bar 2 μm).
C and D. TIRF images of *mcherry-pvdQ* (C) and *pvdQ-mcherry* strains (D). From left to right, brightfield and TIRF images (scale bar 2 μm).

fied fluorescent halos, similar to the distribution detected for periplasmic PVDI (Hannauer *et al*., 2010; Yeterian *et al*., 2010a,b) (Fig. 5A and B). We also used Total Internal Reflection (TIRF) microscopy imaging (Fig. 5C and D), in which the incident light is inclined so that only the cell surface is illuminated. Considering the cell-fractionation findings, the full cell surface displayed in TIRF mode allowed us to visualize a uniform periplasmic localization for both mCHERRY fusions. PvdQ, with mCHERRY fused to either its α- or β-subunit, is therefore uniformly distributed throughout the periplasm.

Discussion

Bacteria are now understood to have a higher degree of intracellular organization than previously thought. Individual proteins are located at particular sites within the bacterial cell and these distribution patterns are often dynamic (Dworkin, 2009; Shapiro *et al*., 2009; Rudner and Losick, 2010). PVDI biosynthesis is a multistep process starting in the cytoplasm and ending in the periplasm and involving at least 11 different proteins. The activities of most of these are now well characterized. However, the bacterial intracellular organization of the sequential steps that lead to mature PVDI and their orchestration *in vivo* remain unknown.

PvdA, a L-ornithine N^{δ}-oxygenase, is one of the initial enzymes in the biosynthetic pathway of PVDI in the cytoplasm (Visca *et al*., 1994; 2007). The N-terminal domain of PvdA has been recently shown to have two overlapping functional regions; an FAD-binding site and an inner membrane anchoring hydrophobic domain (Imperi *et al*., 2008; Meneely *et al*., 2009). In a wild-type context, PvdA was only fully functional and intact when eYFP was fused to its C-terminus. When we fused the N-terminus of PvdA with eYFP, no PVDI was produced and immunoblot analysis indicated there was likely no PvdA protein present in the cells. For the C-terminal fusion protein, we found a high content of eYFP in the membrane fraction after cellular fractionation of the corresponding *pvdA-yfp* strain, as previously reported for wild-type PvdA (Imperi *et al*., 2008). Epifluorescence imaging revealed that the PvdA-YFP fusion protein was not randomly distributed along the inner membrane but instead appeared as a spot at one cell pole. The asymmetric segregation of proteins has been previously reported to be a marker of cellular aging and rejuvenation in bacteria (Lindner *et al*., 2008). However, such process is associated with irreversible protein aggregation, whereas adding PVDI-Fe to bacteria with PvdA-YFP clusters to reverse PVDI biosynthesis led to the disappearance of clustered proteins (Fig. 3D). Thus, the clustering of PvdA appears to be a dynamic process and must involve other functional proteins. As PvdA is involved in the complex sequential addition of peptide building blocks to form a cytoplasmic non-fluorescent PVDI precursor with a myristic acid chain, the

spotted localization of PvdA may reflect the need to compartmentalize this coordinated process in a crowded environment such as the cytoplasm. Indeed, the PvdA patch that we observed might also contain other enzymes required for PVDI biosynthesis in the cytoplasm. The cytoplasmic precursor of PVDI with a myristic acid chain (Gulick and Drake, 2011; Hannauer *et al.*, 2012) would therefore continually pass from one enzyme to another, and never be free in the cytoplasm. This organization would optimize the efficiency of the process by keeping the PVDI precursor close to the membrane and avoiding its dilution into the cytoplasm. Bacterial chemotaxis signal transduction proteins are also organized as protein assembly patches composed of transmembrane chemoreceptors and associated cytoplasmic proteins [for a review, see (Sourjik, 2004)]. Using similar experimental models to those used in our study (Martin *et al.*, 2001; Cantwell *et al.*, 2003; Guvener *et al.*, 2006), immunogold electron microscopy (Harrison *et al.*, 1999), and electron tomography (Briegel *et al.*, 2009), other authors have identified a cluster of proteins located at the cell pole allowing signal transduction from the periplasm to the cytoplasm. As we observed with PvdA, these proteins are not only present at the cell poles; a subset remains in the cytoplasm and the number of spotted cells increases during growth (Martin *et al.*, 2001; Cantwell *et al.*, 2003; Guvener *et al.*, 2006). PvdA promoter activity reaches a peak during the mid-exponential phase, after which it decreases (Putignani *et al.*, 2004). This radical change in PvdA promoter activity thus appears to coincide with the moment we observe the switch from homogeneously distributed proteins to the appearance of patched proteins in cells, and may in turn indicate how this conversion is governed. The significance of the spotted bacterial cells versus the unspotted cells remains unknown, but probably represents the different growing stages of individual bacteria.

During cell division, we found that the clustered PvdA did not relocate to both cell poles; the distribution to the daughter cells was asymmetric, resulting in an old cell pole location. Although asymmetrical division in bacteria remains contentious, there are an increasing number of examples appearing in the literature (for a review, see Shapiro *et al.*, 2002). Whereas genetic information is equally distributed to the daughter cells, surface structures, such as flagella or pili, are preferentially associated at one cell pole and are thus inherited by only one daughter cell. In the pathogenic bacteria *Shigella flexneri* and *Listeria monocytogenes*, the old cell poles accumulate proteins that promote interactions with the host (Goldberg *et al.*, 1993; Smith *et al.*, 1995).

Finally, addition of 10 μM PVDI-Fe to *pvdA-yfp* cells did not result in rapid dissolution of the PvdA-YFP spot; they only started to disappear after a cell-division cycle. This suggests that PVDI-Fe does not regulate the organization of PvdA into spots.

PvdQ is a well-characterized Ntn-hydrolase that removes the myristic chain linked to the precursor PVDI before secretion (Lamont and Martin, 2003; Bokhove *et al.*, 2010; Nadal Jimenez *et al.*, 2010; Gulick and Drake, 2011). When transferred into PAO1 strains, the N-terminal and C-terminal fusion proteins of PvdQ exhibited the full enzymatic activity of PvdQ and produced PVDI at wild-type levels. In contrast with the spotted location of PvdA, PvdQ was uniformly distributed throughout the periplasm. Fluorescent PVDI having no more myristic chain is also detected all over the periplasm by epifluorescence microscopy (Yeterian *et al.*, 2010a). Mutation of the efflux pump PvdRT-OpmQ involved in PVDI secretion across the outer membrane, increases PVDI accumulation in the bacterial periplasm (Hannauer *et al.*, 2010). Together all these data suggest a maturation of PVDI homogeneously distributed throughout the periplasm.

In conclusion, our results suggest that the PVDI cytoplasmic precursor is synthesized through coordinated enzymatic activities localized at the interface between the cytoplasm and the inner membrane of the bacterial old cell pole. This specific cellular localization probably ensures the efficiency of this complex biosynthesis. PvdQ, an enzyme involved in the periplasmic maturation of PVDI, is homogeneously distributed throughout the periplasm like fluorescent PVDI having no more myristic chain (Yeterian *et al.*, 2010a). This homogeneous distribution of PVDI maturation all over the bacterial periplasm probably ensures a secretion of the siderophore across the outer membrane all over the bacterial periphery. Further studies are required to confirm this model and to identify the cell localization of the other enzymes involved in this process.

Experimental procedures

Bacterial strains, plasmids and growth conditions

The *P. aeruginosa* and *Escherichia coli* strains and the plasmids used in this study are listed in Table 1. Bacteria were usually grown in Luria broth [(LB); Difco] medium kept at 37°C. The *P. aeruginosa* strains were grown overnight at 30°C in an iron-deficient succinate medium (composition: 6 g l^{-1} K_2HPO_4, 3 g l^{-1} KH_2PO_4, 1 g l^{-1} $[NH_4]_2SO_4$, 0.2 g l^{-1} $MgSO_4$ $7H_2O$ and 4 g l^{-1} sodium succinate with the pH adjusted to 7.0 by adding NaOH). The antibiotic, gentamicin (50 μg ml^{-1}), was added as required.

Mutant construction

All enzymes for DNA manipulation were purchased from Fermentas and were used in accordance with the manufacturer's instructions. *E. coli* strain TOP10 (Invitrogen) was used as a

Table 1. Strains and plasmids used in this study.

Strain or plasmid	Collection ID	Relevant characteristics	Source or reference
P. aeruginosa strains			
PAO1	PAO1	Wild-type strain	Stover *et al.* (2000)
PAO1*pvdQ*	PAO1*pvdQ*	PAO1; *pvdQ*::pEXGm	Lamont and Martin (2003)
PAO1*pvdA*	PAS158	Derivative of PAO1; Δ*pvdA*, chromosomally integrated	This study
yfp-pvdA	PAS101	Derivative of PAO1; *eyfp-pvdA*, chromosomally integrated	This study
pvdA-yfp	PAS102	Derivative of PAO1; *pvdA-eyfp*, chromosomally integrated	This study
mcherry-pvdQ	PAS065	Derivative of PAO1; *mcherry-pvdQ*, mCHERRY insertion after A23 of PvdQ, chromosomally integrated	This study
pvdQ-mcherry	PAS069	Derivative of PAO1; *pvdQ-mcherry*, chromosomally integrated	This study
E. coli strains			
TOP10		*supE44 DlacU169 (φ80lacZDM15) hsdR17 recA1 endA1 gyrA96 thi-1relA1*	Invitrogen
S17-1		*pro thi hsdR recA*; chromosomal RP4 (Tra+ Tcs Kms Aps); Tpr Smr	Simon *et al.* (1983)
Suicide vector and mutator			
pME3088		Suicide vector; Tc^R; ColE1 replicon; EcoRI KpnI DraII XhoI HindIII polylinker	Voisard *et al.* (1994)
pMEM1		pME3088 *eyfp-pvdA* with 700 bp flanking region relative to *eyfp*	This study
pMEM2		pME3088 *pvdA-eyfp* with 700 bp flanking region relative to *eyfp*	This study
pLG1		pME3088 *mcherry-pvdQ* with 700 bp flanking region relative to *mcherry*	This study
pLG2		pME3088 *pvdQ-mcherry* with 700 bp flanking region relative to *mcherry*	This study
pLG3		pME3088Δ*pvdA*	This study

host strain for all plasmids. PCR, using *iProof* polymerase (Bio-Rad), was used to amplify the genes encoding the fluorescent proteins from the following cDNAs: pCDNA3.1/mCHERRY for mCHERRY and pCDNA3.1/eYFP for eYFP. The DNA fragments from *Pseudomonas* used for cloning were amplified from the PAO1 genomic DNA. Primers used are listed in Table S1 of *Supporting information*. The general procedure consisted of cloning the pME3088 suicide vector (Voisard *et al.*, 1994) into a construct composed of the fluorescent protein encoding DNA flanked by upstream and downstream regions of 700 bp relative to the insertion site. Mutations in the chromosomal genome of *P. aeruginosa* were generated by transferring the suicide vectors from *E. coli* S17-1 into the PAO1 strains and integration of the plasmids into the chromosome, with selection for tetracycline resistance. A second crossing-over event excising the vector was achieved by enrichment for tetracycline-sensitive cells to generate the corresponding mutants (Ye *et al.*, 1995). All gene-replacement mutants were verified by PCR.

PvdA labelled at the N-terminus with eYFP (YFP-PvdA) was derived through three sets of PCRs. The 700 bp region upstream to the PvdA gene, which contains the ATG start codon, was amplified by the primers PvdA1 and PvdA2, which inserted restriction sites for EcoRI and XbaI respectively. The 700 bp downstream region was amplified by the primers PvdA3 and PvdA4, which inserted restriction sites for XhoI and HindIII respectively. The DNA encoding eYFP was amplified by the primers YFP1 and YFP2, which inserted restriction sites for XbaI and XhoI respectively. Following PCR, the amplified 700 bp upstream region was digested by XbaI, the amplified 700 bp downstream region was digested by XhoI, and the amplified DNA encoding eYFP was digested by XbaI and XhoI. After their digestion, all three of these PCR products were ligated in equimolar amounts. The ligation product was used as a DNA template for further amplification with the primers PvdA1 and PvdA4. The PCR product was digested by EcoRI and HindIII, ligated into pME3088, linearized by the same enzymes, to produce pMEM1.

PvdA labelled at the C-terminus with eYFP (PvdA-YFP) was also derived from three sets of PCRs. The 700 bp region upstream relative to the stop codon was amplified by the primers and PvdA6, which inserted restriction sites for EcoRI and XbaI. The 700 bp downstream region containing the stop codon was amplified with primers PvdA7 and PvdA8, which inserted restriction sites for XhoI and HindIII respectively. The eYFP-encoding DNA was amplified with the primers YFP1 and YFP2, which inserted restriction sites for XbaI and XhoI respectively. Following PCR, the amplified 700 bp upstream region was digested by XbaI, the amplified 700 bp downstream region was digested by XhoI, and the amplified DNA encoding eYFP was digested by XbaI and XhoI respectively. After their digestion, all three of these PCR products were ligated in equimolar amounts. The ligation product was used as a template for amplification by primers PvdA5 and PvdA8, and the resulting PCR product was digested by EcoRI and HindIII, cloned into pME3088, linearized by the same enzymes to produce pMEM2.

PvdQ labelled at the N-terminus with mCHERRY (mCHERRY-PvdQ) was derived from three sets of PCRs. The 700 bp upstream region containing the predicted protease I cleavage site (amino acid A23) was amplified with the primers PvdQ1, which inserting a restriction site for EcoRI, and PvdQ2, which inserted a restriction site for XbaI. The 700 bp downstream region starting from the codon of D24 was amplified with the primers PvdQ3, which inserted a restriction site for SalI, and PvdQ4, which inserted a restriction for HindIII. The DNA encoding mCHERRY was amplified with the primers, mCHERRY1, which inserted a restriction site for XbaI, and mCHERRY2, which inserted a restriction site for SalI. Following PCR, the amplified 700 bp upstream region was digested by XbaI, the amplified 700 bp downstream region was digested by SalI, and the amplified DNA encoding mCHERRY was digested by XbaI and SalI. After their diges-

tion, all three of these PCR products were ligated in equimolar amounts. The ligation product was used as a DNA template for further amplification with the primers PvdQ1 and PvdQ4, and the resulting PCR product was digested by EcoRI and HindIII, ligated into pME3088, linearized by the same enzymes, to produce pLG1.

PvdQ labelled at the C-terminus with mCHERRY (PvdQ-mCHERRY) was also derived from three sets of PCRs. The 700 bp region upstream to the TGA stop codon was amplified using the primers PvdQ5, which inserted a restriction site for EcoRI, and PvdQ6, which inserted a restriction site for and XbaI. The downstream region containing the stop codon was amplified with primers PvdQ7, which inserted a restriction site for SalI, and primer PvdQ8, which inserted a restriction site for HindIII. DNA encoding mCHERRY was amplified with the primers mCHERRY1, which inserted a 3′ restriction site for XbaI, and mCHERRY2, which inserted a 5′ restriction site for SalI. Following PCR, the amplified 700 bp upstream region was digested by XbaI, the amplified 700 bp downstream was digested by SalI, and the amplified DNA encoding mCHERRY was digested by ClaI and SalI. All three of these digested PCR products were then ligated in equimolar amounts to generate the DNA template for amplification with primers PvdQ5 and PvdQ8. The resulting PCR product was digested with EcoRI and HindIII, ligated into pME3088, and was then linearized with the same enzymes to yield pLG2.

To generate a suicide vector for *pvdA* deletion in PAO1 (PAO1*pvdA*) strain, two regions of 700 bp upstream and downstream of *pvdA* were generated by PCR using primers PvdA1 and PvdA9, inserting EcoRI and XbaI restriction sites, and PvdA10 and PvdA8, inserting XbaI and HindIII respectively. The two fragments were digested by XbaI and ligated to yield the DNA template for amplification with primers PvdA1 and PvdA8. The PCR product was digested with EcoRI and HindIII and ligated into pME3088, linearized with the same enzymes, giving pLG3.

Growth and quantification of PVDI production

Cells were cultured overnight in LB media kept at 37°C. Cells were pelleted and washed once with one volume of succinate media and then resuspended to reach a final concentration of 0.1 OD_{600} ml^{-1}. Two hundred microlitres of the suspension were distributed into 96 well plates (Greiner, PS-microplate flat bottom). Plates were then incubated at 30°C and agitated in a Tecan microplate reader (Infinite M200, Tecan) for measurements of OD_{600} and OD_{400} every 30 min over 35 h. Each measurement represented a mean taken from six replicates.

Iron uptake assays

PVDI-^{55}Fe (0.25 Ci $mmol^{-1}$) was prepared as previously described (Schalk *et al*., 2001), with a fourfold excess of PVDI over iron. The uptake assays were carried out as described previously (Schalk *et al*., 2001). An overnight culture in iron-limited medium was harvested and the bacteria prepared at an OD_{600} of 1 in 50 mM Tris-HCl (pH 8.0) and incubated at 37°C. Transport assays were initiated by adding 100 nM of PVDI-^{55}Fe. Aliquots (100 µl) of the suspension were removed at different times, filtered, washed with 3 ml 50 mM Tris-HCl (pH 8.0) and the retained radioactivity was counted. The experiment was repeated with cells that had previously been treated with 200 µM carbonyl cyanide m-chlorophenylhydrazone (CCCP), a protonophore that inhibits iron uptake (Clément *et al*., 2004).

Biofilm quantification (Siroy et al*., 2006)*

Cells were cultured in LB media overnight at 37°C. Cells were pelleted and washed once with one volume of succinate media and were then resuspended to a final concentration of 0.05 OD_{600} ml^{-1}. Three millilitres of the suspension were distributed in triplicate into a six-well plate (Greiner, TC-plate CELLSTAR). Plates were then incubated at 30°C over 24 h on a rocker shaker. For crystal-violet treatment, culture supernatants were carefully removed, and the biofilm was washed twice with sterile water. One millilitre of 0.5% crystal violet was added and left in contact for 15 min at room temperature with gentle agitation. After removal of the solution, the biofilm was washed twice with sterile water before elution of crystal violet by 1 ml of ethanol. The biofilm was then quantified by measuring the absorbance at 570 nm of either the directly eluted crystal violet or of an appropriate dilution for accurate quantification.

Immunoblot analysis

We subjected 0.25 OD_{600} units of cells grown in succinate media to SDS-PAGE. Proteins were transferred onto nitrocellulose membranes by electroblotting (Bio-Rad). The nitrocellulose membranes were then blocked by incubation for 1 h in blocking solution [phosphate-buffered saline (PBS), pH 7.6, 10% dried milk powder] followed by incubation in blocking buffer supplemented with primary anti-PvdQ antibodies (1:1000 dilution), anti-GFP antibodies (1:10 000 dilution), or anti-DsRed antibodies (1:100 dilution, Ozyme). Membranes were then incubated in PBS (pH 7.6, 0.1% Tween) supplemented with a secondary antibody of IRDye 800CW donkey anti-rabbit IgG (1:10 000 dilution, Clinisciences). Antibody binding was detected with an Odyssey Imager (LI-COR Biosciences).

Cell fractionation

Periplasm and cytoplasm fractions were prepared as previously described (Nader *et al*., 2011). Fifty millilitres of bacterial cultures grown overnight in succinate medium were centrifuged to obtain a cell pellet, which was washed twice with 50 mM Tris-HCl pH 8.0 and then resuspended in 1.5 ml of buffer A (200 mM Tris-HCl, pH 8.0, 20% sucrose). Spheroplasts were obtained by adding 15 µl of 100 mg ml^{-1} lysozyme (Euromedex) to the suspension and shaking the mixture gently at 4°C for 1 h. The suspension was then centrifuged (15 min at 6700 *g*) to obtain the spheroplast pellet and the periplasmic fraction (the supernatant). Spheroplast pellets were washed with 500 µl of buffer A, and resuspended in 1.5 ml of cold water by vortexing; the resulting suspension was incubated for 1 h at 37°C with benzonase (1 µl of a 50-fold dilution of benzonase $\geq$ 250 units μl^{-1} from Sigma). The cytoplasmic fractions were isolated by ultracentrifugation

(40 min at 120 000 *g*). Pellets were resuspended in about 1.5 ml of buffer A. Two hundred microlitres of each fraction were distributed into a 96-well plate and the fluorescence was measured in a Tecan microplate reader (Infinite M200, Tecan) using the following excitation/emission wavelengths: 400 nm/450 nm for PVDI, 514 nm/527 nm for eYFP, and 570 nm/610 nm for mCHERRY.

Fluorescence microscopy imaging

Samples were prepared from strains cultured overnight in succinate media. Cultures were washed by succinate media and appropriately diluted in the same media. Five microlitres of cell suspension were spotted on a glass slide that was freshly coated with 1% agarose made in minimal media, and covered with a coverslip. TIRF images were acquired with an Observer.A1 (Zeiss) equipped with a Plan Fluar objective (NA: 1.45, Zeiss) and a Cascade II 512 EMCCD camera (photometrics). The imaging system was operated using the software, VisiView 1.7.4 (Visitron Systems GmbH). mCHERRY was excited by exposure to a laser of 561 nm wavelength with a visitron VisiTIRF system. Fluorescence signals were aquired using an appropriate filter cube. To determine the pole location of the patched *pvdA-yfp* during bacterial growth, cell division of the strain – grown twice in succinate media during the exponential phase – was monitored. Cells were spotted onto slides coated with agarose, which was dissolved in succinate media. Cells were imaged after 0, 1 and 2 h incubation periods at 30°C with a Nikon 50i (objective: CFI Achroplan 100 × A ON 1.25 DT 0.18) microscope equipped with a numeric 12 bits DS-Fi1 camera. For fluorescence imaging of eYFP, the filter GFP-3035B (excitation 472 ± 32 nm, emission 520 ± 35 nm, dichroic filter 502–730 nm) was used. Images were captured using the imaging software, NIS elements. Images were minimally processed with Image-J_{NIH} software (Abramoff *et al*., 2004).

Acknowledgements

This work was partly funded by the Centre National de la Recherche Scientifique, by grants from the Centre International de Recherche au Frontière de la Chimie (FRC), from the ANR (Agence Nationale de Recherche, ANR-08-BLAN-0315-01), as well as from the Deutsche Forschungsgemeinschaft (FOR 929 and SFB 746). We thank Prof. Bruno Chatton, for access to the Odyssey Imager. We thank Prof. Etienne Weiss for the plasmids encoding mCHERRY and eYFP and Prof. Wim Quax for anti-PvdQ antibodies.

References

Abramoff, M.D., Magalhaes, P.J., and Ram, S.J. (2004) Image processing with Image J. *Biophotonics Int* **11:** 36–42.

Ackerley, D.F., Caradoc-Davies, T.T., and Lamont, I.L. (2003) Substrate specificity of the nonribosomal peptide synthetase PvdD from *Pseudomonas aeruginosa*. *J Bacteriol* **185:** 2848–2855.

Bokhove, M., Jimenez, P.N., Quax, W.J., and Dijkstra, B.W. (2010) The quorum-quenching N-acyl homoserine lactone acylase PvdQ is an Ntn-hydrolase with an unusual substrate-binding pocket. *Proc Natl Acad Sci USA* **107:** 686–691.

Boukhalfa, H., and Crumbliss, A.L. (2002) Chemical aspects od siderophore mediated iron transport. *Biometals* **15:** 325–339.

Braun, V., and Hantke, K. (2011) Recent insights into iron import by bacteria. *Curr Opin Chem Biol* **15:** 328–334.

Briegel, A., Ortega, D.R., Tocheva, E.I., Wuichet, K., Li, Z., Chen, S., *et al*. (2009) Universal architecture of bacterial chemoreceptor arrays. *Proc Natl Acad Sci USA* **106:** 17181–17186.

Cantwell, B.J., Draheim, R.R., Weart, R.B., Nguyen, C., Stewart, R.C., and Manson, M.D. (2003) CheZ phosphatase localizes to chemoreceptor patches via CheA-short. *J Bacteriol* **185:** 2354–2361.

Clément, E., Mesini, P.J., Pattus, F., Abdallah, M.A., and Schalk, I.J. (2004) The binding mechanism of pyoverdin with the outer membrane receptor FpvA in *Pseudomonas aeruginosa* is dependent on its iron-loaded status. *Biochemistry* **43:** 7954–7965.

Demange, P., Wendenbaum, S., Linget, C., Mertz, C., Cung, M.T., Dell, A., and Abdallah, M.A. (1990) Bacterial siderophores: structure and NMR assigment of pyoverdins PaA, siderophores of *Pseudomonas aeruginosa* ATCC 15692. *Biol Met* **3:** 155–170.

Dworkin, J. (2009) Cellular polarity in Prokaryotic organisms. *Cold Spring Harb Perspect Biol* **1:** a003368.

Goldberg, M.B., Barzu, O., Parsot, C., and Sansonetti, P.J. (1993) Unipolar localization and ATPase activity of IcsA, a *Shigella flexneri* protein involved in intracellular movement. *J Bacteriol* **175:** 2189–2196.

Greenwald, J., Hoegy, F., Nader, M., Journet, L., Mislin, G.L.A., Graumann, P.L., and Schalk, I.J. (2007) Real-time FRET visualization of ferric-pyoverdine uptake in *Pseudomonas aeruginosa*: a role for ferrous iron. *J Biol Chem* **282:** 2987–2995.

Gulick, A.M., and Drake, E.J. (2011) Structural characterization and high-throughput screening of inhibitors of PvdQ, an NTN Hydrolase involved in pyoverdine synthesis. *ACS Chem Biol* **6:** 1277–1286.

Guvener, Z.T., Tifrea, D.F., and Harwood, C.S. (2006) Two different *Pseudomonas aeruginosa* chemosensory signal transduction complexes localize to cell poles and form and remould in stationary phase. *Mol Microbiol* **61:** 106–118.

Hannauer, M., Yeterian, E., Martin, L.W., Lamont, I.L., and Schalk, I.J. (2010) Secretion of newly synthesized pyoverdine by *Pseudomonas aeruginosa* involves an efflux pump. *FEBS Lett* **584:** 4751–4755.

Hannauer, M., Schäfer, M., Hoegy, F., Gizzi, P., Wehrung, P., Mislin, G.L.A., *et al*. (2012) Biosynthesis of the pyoverdine siderophore of *Pseudomonas aeruginosa* involves precursors with a myristic or a myristoleic acid chain. *FEBS Lett* **586:** 96–101.

Harrison, D.M., Skidmore, J., Armitage, J.P., and Maddock, J.R. (1999) Localization and environmental regulation of MCP-like proteins in *Rhodobacter sphaeroides*. *Mol Microbiol* **31:** 885–892.

Hider, R.C., and Kong, X. (2011) Chemistry and biology of siderophores. *Nat Prod Rep* **27:** 637–657.

Imperi, F., Putignani, L., Tiburzi, F., Ambrosi, C., Cipollone, R., Ascenzi, P., and Visca, P. (2008) Membrane-association determinants of the omega-amino acid monooxygenase PvdA, a pyoverdine biosynthetic enzyme from *Pseudomonas aeruginosa*. *Microbiology* **154:** 2804–2813.

Lamont, I.L., and Martin, L.W. (2003) Identification and characterization of novel pyoverdine synthesis genes in *Pseudomonas aeruginosa*. *Microbiology* **149:** 833–842.

Lewenza, S., Gardy, J.L., Brinkman, F.S., and Hancock, R.E. (2005) Genome-wide identification of *Pseudomonas aeruginosa* exported proteins using a consensus computational strategy combined with a laboratory-based PhoA fusion screen. *Genome Res* **15:** 321–329.

Lindner, A.B., Madden, R., Demarez, A., Stewart, E.J., and Taddei, F. (2008) Asymmetric segregation of protein aggregates is associated with cellular aging and rejuvenation. *Proc Natl Acad Sci USA* **105:** 3076–3081.

McMorran, B.J., Kumara, H.M., Sullivan, K., and Lamont, I.L. (2001) Involvement of a transformylase enzyme in siderophore synthesis in *Pseudomonas aeruginosa*. *Microbiology* **147:** 1517–1524.

Martin, A.C., Wadhams, G.H., and Armitage, J.P. (2001) The roles of the multiple CheW and CheA homologues in chemotaxis and in chemoreceptor localization in *Rhodobacter sphaeroides*. *Mol Microbiol* **40:** 1261–1272.

Meneely, K.M., Barr, E.W., Bollinger, J.M., Jr, and Lamb, A.L. (2009) Kinetic mechanism of ornithine hydroxylase (PvdA) from *Pseudomonas aeruginosa*: substrate triggering of O2 addition but not flavin reduction. *Biochemistry* **48:** 4371–4376.

Meyer, J.M., and Abdallah, M.A. (1978) The fluorescent pigment of *Pseudomonas fluorescens*: biosynthesis, purification and physicochemical properties. *J Gen Microbiol* **107:** 319–328.

Mossialos, D., Ochsner, U., Baysse, C., Chablain, P., Pirnay, J.P., Koedam, N., *et al*. (2002) Identification of new, conserved, non-ribosomal peptide synthetases from fluorescent pseudomonads involved in the biosynthesis of the siderophore pyoverdine. *Mol Microbiol* **45:** 1673–1685.

Nadal Jimenez, P., Koch, G., Papaioannou, E., Wahjudi, M., Krzeslak, J., Coenye, T., *et al*. (2010) Role of PvdQ in *Pseudomonas aeruginosa* virulence under iron-limiting conditions. *Microbiology* **156:** 49–59.

Nader, M., Journet, L., Meksem, A., Guillon, L., and Schalk, I.J. (2011) Mechanism of ferrisiderophore uptake by *Pseudomonas aeruginosa* outer membrane transporter FpvA: no diffusion channel formed at any time during ferrisiderophore uptake. *Biochemistry* **50:** 2530–2540.

Ochsner, U.A., Wilderman, P.J., Vasil, A.I., and Vasil, M.L. (2002) GeneChip expression analysis of the iron starvation response in *Pseudomonas aeruginosa*: identification of novel pyoverdine biosynthesis genes. *Mol Microbiol* **45:** 1277–1287.

Oinonen, C., and Rouvinen, J. (2000) Structural comparison of Ntn-hydrolases. *Protein Sci* **9:** 2329–2337.

Putignani, L., Ambrosi, C., Ascenzi, P., and Visca, P. (2004) Expression of L-ornithine Ndelta-oxygenase (PvdA) in fluorescent *Pseudomonas* species: an immunochemical and in silico study. *Biochem Biophys Res Commun* **313:** 245–257.

Ravel, J., and Cornelis, P. (2003) Genomics of pyoverdine-mediated iron uptake in pseudomonads. *Trends Microbiol* **11:** 195–200.

Rudner, D.Z., and Losick, R. (2010) Protein subcellular localization in bacteria. *Cold Spring Harb Perspect Biol* **2:** a000307.

Schalk, I.J. (2008) Metal trafficking via siderophores in Gram-negative bacteria: specificities and characteristics of the pyoverdine pathway. *J Inorg Biochem* **102:** 1159–1169.

Schalk, I.J., Hennard, C., Dugave, C., Poole, K., Abdallah, M.A., and Pattus, F. (2001) Iron-free pyoverdin binds to its outer membrane receptor FpvA in *Pseudomonas aeruginosa*: a new mechanism for membrane iron transport. *Mol Microbiol* **39:** 351–360.

Shapiro, L., McAdams, H.H., and Losick, R. (2002) Generating and exploiting polarity in bacteria. *Science* **298:** 1942–1946.

Shapiro, L., McAdams, H.H., and Losick, R. (2009) Why and how bacteria localize proteins. *Science* **326:** 1225–1228.

Simon, R., Priefer, U., and Puhler, A. (1983) A broad host range mobilization system for in vivo genetic engineering: transposon mutagenesis in Gram Negative bacteria. *Nat Biotechnol* **1:** 784–791.

Sio, C.F., Otten, L.G., Cool, R.H., Diggle, S.P., Braun, P.G., Bos, R., *et al*. (2006) Quorum quenching by an N-acyl-homoserine lactone acylase from *Pseudomonas aeruginosa* PAO1. *Infect Immun* **74:** 1673–1682.

Siroy, A., Cosette, P., Seyer, D., Lemaitre-Guillier, C., Vallenet, D., Van Dorsselaer, A., *et al*. (2006) Global comparison of the membrane subproteomes between a multidrug-resistant *Acinetobacter baumannii* strain and a reference strain. *J Proteome Res* **5:** 3385–3398.

Smith, G.A., Portnoy, D.A., and Theriot, J.A. (1995) Asymmetric distribution of the *Listeria monocytogenes* ActA protein is required and sufficient to direct actin-based motility. *Mol Microbiol* **17:** 945–951.

Sourjik, V. (2004) Receptor clustering and signal processing in *E. coli* chemotaxis. *Trends Microbiol* **12:** 569–576.

Stover, C.K., Pham, X.Q., Erwin, A.L., Mizoguchi, S.D., Warrener, P., Hickey, M.J., *et al*. (2000) Complete genome sequence of *Pseudomonas aeruginosa* PAO1, an opportunistic pathogen. *Nature* **406:** 959–964.

Vandenende, C.S., Vlasschaert, M., and Seah, S.Y. (2004) Functional characterization of an aminotransferase required for pyoverdine siderophore biosynthesis in *Pseudomonas aeruginosa* PAO1. *J Bacteriol* **186:** 5596–5602.

Visca, P., Ciervo, A., and Orsi, N. (1994) Cloning and nucleotide sequence of the pvdA gene encoding the pyoverdin biosynthetic enzyme L-ornithine N5-oxygenase in *Pseudomonas aeruginosa*. *J Bacteriol* **176:** 1128–1140.

Visca, P., Imperi, F., and Lamont, I.L. (2007) Pyoverdine siderophores: from biogenesis to biosignificance. *Trends Microbiol* **15:** 22–30.

Voisard, C., Bull, C., Keel, C., Laville, J., Maurhofer, M., Schnider, U., *et al*. (1994) Biocontrol of root diseases by *Pseudomonas fluorescens* CHAO: current concepts and experimental approaches. In *Molecular Ecology of Rhizosphere Microorganisms*. O'Gara, F., Dowling, D.N., and Boesten, B. (eds). Weinheim, Germany: VCH, pp. 67–89.

Voulhoux, R., Filloux, A., and Schalk, I.J. (2006) Role of the TAT System in the pyoverdine-mediated iron acquisition in *Pseudomonas aeruginosa*. *J Bacteriol* **188:** 3317–3323.

Wang, L., Zhang, C., Gong, F., Li, H., Xie, X., Xia, C., *et al*. (2011) Influence of *Pseudomonas aeruginosa pvdQ* gene on altering antibiotic susceptibility under swarming conditions. *Curr Microbiol* **63:** 377–386.

Ye, R.W., Haas, D., Ka, J.O., Krishnapillai, V., Zimmermann, A., Baird, C., and Tiedje, J.M. (1995) Anaerobic activation of the entire denitrification pathway in *Pseudomonas aeruginosa* requires Anr, an analog of Fnr. *J Bacteriol* **177:** 3606–3609.

Yeterian, E., Martin, L.W., Guillon, L., Journet, L., Lamont, I.L., and Schalk, I.J. (2010a) Synthesis of the siderophore pyoverdine in *Pseudomonas aeruginosa* involves a periplasmic maturation. *Amino Acids* **38:** 1447–1459.

Yeterian, E., Martin, L.W., Lamont, I.L., and Schalk, I.J. (2010b) An efflux pump is required for siderophore recycling by *Pseudomonas aeruginosa*. *Environ Microbiol Rep* **2:** 412–418.

Supporting information

Additional Supporting Information may be found in the online version of this article:

Fig. S1. Time-dependent uptake of PVDI-^{55}Fe. Panel A represents the kinetics for PAO1 in the presence and absence of CCCP (kinetics in orange and red respectively) and *pvdA-yfp* (blue) in the absence of CCCP. Panel B represents the kinetics for PAO1 in the presence and absence of CCCP (kinetics in orange and red respectively), PAO1*pvdQ* (brown), *mcherry-pvdQ* (green) and *pvdQ-mcherry* (yellow), all in the absence of CCCP. Cells at an OD_{600} of 1 were incubated for 15 min at 37°C in 50 mM Tris-HCl (pH 8.0) before the initiation of transport assays by the addition of 100 nM PVDI-^{55}Fe. Samples (100 μl) of the suspension were removed at various times and filtered, and the radioactivity retained was counted. The results are expressed as picomoles of PVDI-^{55}Fe transported per millilitre of cells at an OD_{600} of 1. The experiment was repeated with the protonophore CCCP at a concentration of 200 μM (only the kinetics for PAO1 are represented).

Fig. S2. Biofilm quantification by violet crystal formed by *P. aeruginosa* PAO1, PAO1*pvdQ*, *mcherry-pvdQ* and *pvdQ-mcherry* strains. Biofilms formed by cultures grown for 24 h in 6-well plates on a rocker shaker were stained by violet crystal (A) and the quantity of crystal violet was evaluated by OD_{570} measurements upon elution by ethanol.

Fig. S3. Immunoblot analysis of cellular fractionations of PAO1, *mcherry-pvdQ* and *pvdQ-mcherry* strains. Equivalent volumes of periplasmic (P), cytoplasmic (C) and membrane (M) fractions were loaded onto SDS-PAGE for protein separation. Proteins were blotted onto nitrocellulose membrane and PvdQ was detected using anti-PvdQ antibodies Molecular weight (MW) marker bands are indicated on the left.

Table S1. Oligonucleotides used in this study. Restriction sites are underlined.

Please note: Wiley-Blackwell are not responsible for the content or functionality of any supporting materials supplied by the authors. Any queries (other than missing material) should be directed to the corresponding author for the article.